Industrial Crops & Products 240 (2026) 122611

Contents lists available at ScienceDirect

Industrial Crops & Products

journal homepage: www.elsevier.com/locate/indcrop

Propagation method and planting density influence canopy developmental transition and biomass productivity in *Miscanthus* × *giganteus*

Jung Woo Lee [a,b,1], Kayla Marie Vittore [a,1], Nictor Namoi [a,b,c], Soonho Hwang [a], DoKyoung Lee [a,b,c,d,*]

[a] Department of Crop Sciences, University of Illinois at Urbana-Champaign, Urbana, IL 61801, USA
[b] DOE Center for Advanced Bioenergy and Bioproducts Innovation, University of Illinois at Urbana-Champaign, Urbana, IL 61801, USA
[c] Agroecosystem Sustainability Center, Institute for Sustainability, Energy, and Environment, University of Illinois at Urbana-Champaign, Urbana, IL 61801, USA
[d] Environmental Science Division, Argonne National Laboratory, 9700 S. Cass Ave, Lemont, IL 60439, USA

ARTICLE INFO

Keywords:
Biomass
Propagation
Planting Density
Miscanthus x giganteus
Bioenergy Crop

ABSTRACT

Understanding how establishment practices influence the mechanisms underlying *Miscanthus* × *giganteus* (miscanthus) productivity and canopy development is critical for optimizing management. Data was collected during the juvenile (2011–2013) and mature (2024) phases of a long-term field experiment established in Urbana, Illinois, to evaluate the effects of propagation method (plug propagation [PP] and rhizome propagation [RP]), planting density (1.0, 0.75, and 0.25 plants m^{-2}), and nitrogen application (0 and 67 kg N ha^{-1}) on end-of-season biomass yield, tiller mass, tiller density, and tiller height. Linear regression models identified the dominant predictors of yield across stand ages and management regimes. Planting density, nitrogen (N) application, and propagation method significantly influenced early yield and canopy development. During the juvenile phase, biomass yield was driven by tiller density due to canopy expansion; in the mature phase, yield became driven by tiller mass. The PP plots produced higher tiller density than the RP plots, resulting in faster canopy closure and higher juvenile-phase yields. Rhizome-propagated (RP) plots produced lower tiller density, but individual tillers were 3.3–6.4 g $tiller^{-1}$ heavier than PP tillers. After the canopy reached equilibrium, the PP and RP yields were similar because greater RP tiller mass compensated for its lower tiller density. Higher planting density resulted in greater yield and tiller density during the second year (2012), but this effect was absent from the third year (2013) onward. In the juvenile phase, N fertilization enhanced yield by 1.6–3.4 Mg ha^{-1}. Initiating fertilization in 2013 on unfertilized plots produced biomass similar to that in fertilized plots, suggesting yield recovery in the mature phase. These findings revealed that establishment strategies, including propagation method and planting density, influence juvenile miscanthus canopy development and productivity, transitioning from tiller-density- to mass-dominated yields, but not mature phase productivity.

1. Introduction

The twin demands for increasing energy production and mitigating greenhouse gas (GHG) emissions have intensified efforts to transition from conventional fossil fuels to biofuel alternatives. In response, the U. S. government launched the Sustainable Aviation Fuel (SAF) Grand Challenge to produce 132 billion liters (35 billion gallons) of SAF annually by 2050 (U.S. Department of Energy, 2021). Meeting this goal will require a reliable annual supply of renewable biomass feedstock; purpose-grown energy crop species are projected to play a central role in achieving supply goals (U.S. Department of Energy; U.S. Department of Transportation; U.S. Department of Agriculture, 2022). Herbaceous species such as *Panicum virgatum* (switchgrass), *Sorghum bicolor* (sorghum), *Saccharum spp.* (energy cane), and *Miscanthus* × *giganteus* are leading energy crop species expected to contribute 345 million dry tons of biomass annually (U.S. Department of Energy, 2024). *Miscanthus* × *giganteus* (hereafter miscanthus) is a promising purpose-grown energy crop because of its high biomass yield potential, averaging between 15.3 and 24.7 Mg ha^{-1} in dry biomass yield depending on the growing conditions (Lee et al., 2018). Moreover, miscanthus has high nitrogen (N),

* Corresponding author at: Department of Crop Sciences, University of Illinois at Urbana-Champaign, Urbana, IL 61801, USA.
E-mail address: leedk@illinois.edu (D.K. Lee).
[1] These authors equally contributed to this work

https://doi.org/10.1016/j.indcrop.2025.122611
Received 29 October 2025; Received in revised form 26 November 2025; Accepted 29 December 2025
Available online 17 January 2026

water, and radiation use efficiencies while also generating significant ecosystem services (Cadoux et al., 2012; Dohleman and Long, 2009; Kane et al., 2023; Maughan et al., 2012; Sharma et al., 2022; Studt et al., 2021; VanLoocke et al., 2012). Given these advantages, miscanthus is projected to hold the second-largest market share of US agricultural-land biomass resources, expected to supply 110 million dry tons of biomass for SAF production (U.S. Department of Energy, 2024).

The miscanthus growth cycle follows three main phases: (1) the establishment/yield-building phase (also called juvenile), when end-of-season biomass increases over 2–4 years; (2) the maturity phase, when yields peak and stabilize for 5–11 years; and (3) the reduced-yield phase, when yields gradually decline (Anderson et al., 2011; Tejera et al., 2022). Juvenile miscanthus prioritizes expanding lateral growth and increasing the tiller density per unit area, but is more vulnerable to environmental stresses. This phase is marked by aggressive rhizome expansion and tillering. In contrast, mature miscanthus prioritizes stress tolerance (Anderson et al., 2011; Tejera et al., 2021). Once fully mature, the established rhizomes compete for space and nutrients, resulting in stabilized tiller density between years (Christian et al., 2008; Clifton-Brown and Lewandowski, 2002; Lee et al., 2017), although weather conditions may influence tiller density within a growing year (Namoi et al., 2024). In this paper, we refer to the stabilized tiller density between years as the canopy density equilibrium. The time needed to accomplish canopy density equilibrium, and thus maturity, is affected by propagation techniques, planting density, N management, and site conditions. These factors shape early establishment and affect the rate at which the stand reaches maturity, ultimately determining long-term productivity (Fig. 1) (Tejera et al., 2021, 2019; Lewandowski et al., 2000).

Miscanthus is a sterile plant typically propagated through two primary asexual methods: rhizome (hereafter RP) and plug propagation (hereafter PP). The RP method uses underground stems obtained from dormant miscanthus stands and is currently the predominant propagation method (Boersma and Heaton, 2014a; Xue et al., 2015). Rhizome propagation can be cost- and labor-intensive during large-scale stand establishment compared to sexual propagation methods, which are common for other seed-producing crops. Moreover, RP is constrained by a minimum size requirement of 15–25 g per planting unit, limiting the number of viable units obtainable from excavated rhizomes (Atkinson, 2009; Boersma and Heaton, 2014b; Vermerris, 2008). In contrast, PP involves pre-planting rhizomes in a controlled environment to generate small miscanthus “plugs”. Smaller rhizome planting units than RP can be utilized, increasing the amount of planting material. Additionally, PP miscanthus has higher, more consistent establishment and regrowth rates than RP miscanthus (Boersma and Heaton, 2014b; Ouattara et al., 2020). The PP method is, nonetheless, more costly than the RP due to the added expense of greenhouse management during the 2–3 months preceding PP transplanting (Xue et al., 2015). Although RP and PP miscanthus may vary in developmental morphology and growth strategies, a previous field evaluation reported that biomass yield in juvenile miscanthus is comparable between methods (Boersma and Heaton, 2014a).

Planting density is a critical factor in agronomy that can affect plant growth and yield across many cropping systems (Zhou et al., 2025, 2023; Sanderson and Reed, 2000; Assefa et al., 2016). Different planting densities can regulate branching architecture and photoassimilate partitioning by altering the regulation of hormone-related gene expression (Zhou et al., 2025, 2023). Density-based growth regulation is fundamentally caused by competition for resources with neighboring plants (Villalobos and Fereres, 2016). In a cropping monoculture, the density-based growth regulation results in the previously described canopy density equilibrium. Therefore, planting density is also a key determinant of miscanthus establishment, affecting both the time to canopy density equilibrium and the time to reach peak biomass yield. Miscanthus stands planted at higher densities achieve higher juvenile yields and reach peak productivity sooner, with the consequence of higher propagation costs (Lewandowski et al., 2000; Miguez et al., 2008). Therefore, determining the optimal planting density for miscanthus with different propagation methods is essential to balance establishment costs with potential profitability. The typical planting density recommendation for miscanthus is 1 m^{-1} (Lee et al., 2018; Lewandowski et al., 2000; Heaton et al., 2008). Higher planting densities are considered less cost-effective (Lewandowski et al., 2000; Aslan-Sungur (Rojda) et al., 2025). However, there are potential advantages to higher planting densities if changes to propagule production or planting could lower the cost per propagule (Xue et al., 2015; Aslan-Sungur (Rojda) et al., 2025). If lower costs are achieved, producers would want to know whether higher planting density provides a yield benefit and if that benefit endures in a long-term perennial system. To our knowledge, past studies on miscanthus planting density effects have only been conducted in Europe (Lewandowski et al., 2000; Miguez et al., 2008; Danalatos et al., 2007), where both the growing season length and miscanthus clone selection differ from the Midwestern U.S (Lee et al., 2017; Boersma and Heaton, 2014a). Moreover, no study has explored the potential synergies or trade-offs arising from different

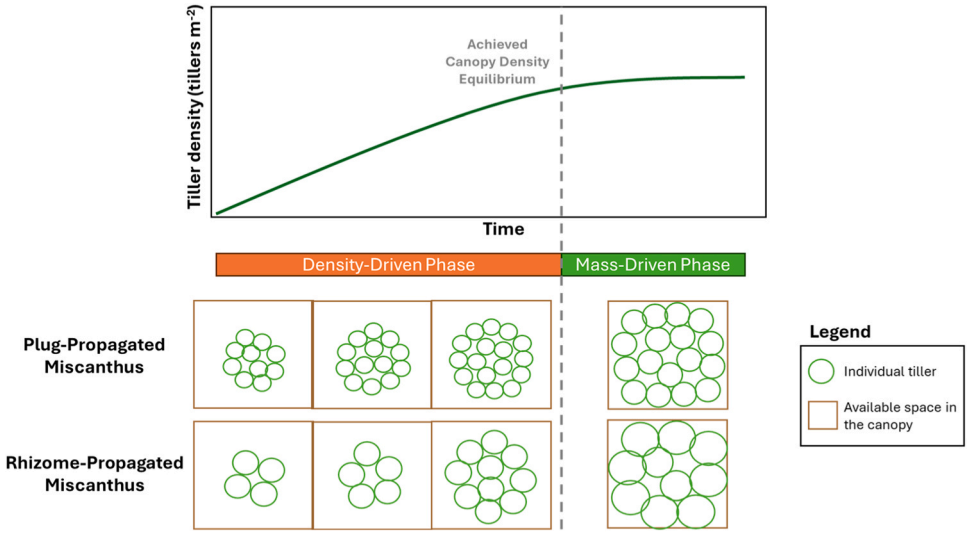

Fig. 1. Schematic summarizing how miscanthus transitions from a density-driven yield in the early juvenile phase to a mass-driven yield in the later juvenile and mature phases. Green circles represent individual tillers from a single miscanthus crown. Brown boxes represent a space allotment for the single miscanthus crown. The brown box area would vary between planting density treatments (0.25 m^2, 0.75 m^2, and 1 m^2 between plants).

planting densities and propagation methods combined with N fertilization during the juvenile phase. Understanding the potential interactions of these factors on miscanthus performance can inform planting decisions to accelerate the stand achieving canopy density equilibrium and subsequently peak productivity.

This study analyzed data from miscanthus stands at opposite ends of its lifecycle for the effects of propagation method, planting density, and N fertilization: the juvenile phase (1–3 years after planting) and the mature phase (~ 13 years after planting, at or beyond peak productivity). The aim was to evaluate how stand establishment strategies influenced miscanthus biomass yield in both the juvenile and mature phases. Specifically, the objectives were to: (i) assess how propagation method and planting density affect end-of-season biomass yield and yield components (tiller density, weight, and height) in juvenile miscanthus, (ii) evaluate the role of nitrogen (N) in modulating yield responses, and (iii) examine the potential long-term impact of establishment methods on productivity in mature miscanthus.

2. Materials and methods

2.1. Site description and experimental design

The field research plots were established in 2011 at the University of Illinois Energy Farm (40.0678333 N, −88.2008583 W) in Urbana, IL, on a Catlin silt loam soil (Fine-silty, mixed, superactive, mesic Oxyaquic Argiudolls). Soil data for the 0–15 cm and 15–30 cm depths before the planting included soil organic matter (3.0 % and 2.3 %), pH (6.35 and 6.25), NH_4-N (8.63 and 7.07 mg kg^{-1}), NO_3-N (5.22 and 3.10 mg kg^{-1}), P (13.2 and 35.2 mg kg^{-1}), and K (92.8 and 163.7 mg kg^{-1}). Biomass yield and yield component data were collected in the 2011–2013 growing seasons during the juvenile phase, and in the 2024 growing season during the mature phase. Precipitation and temperature data corresponding to these data collection periods are compared to the region's 30-year average (1991–2020) in Fig. 2. Growing conditions were consistent during the juvenile phase of the experiment, except in 2012, which experienced drought conditions from warmer monthly average temperatures from January through July (Fig. 2a) and 29 % lower total annual precipitation than the long-term average (Fig. 2b). In the 2024 growing season, monthly temperatures were similar to the long-term average (Fig. 2c), but the total annual precipitation was 23 % higher than the long-term average (Fig. 2d).

The 'Illinois' clone of miscanthus (Chae et al., 2013; Dalton, 2013) was used in this trial. Rhizomes were excavated from the University of Illinois Turf and Ornamental Research Center (Urbana, IL) and segmented into ~25 g units for planting (Maughan et al., 2012; Heaton et al., 2008). Commercially produced plugs, also derived from the 'Illinois' clone of miscanthus, were purchased from New Energy Farms (Leamington, ON, Canada), where they generated plugs using a proprietary technique analogous to that described by Boersma and Heaton (2012). Each propagule (rhizome or plug) was hand-planted in spring 2011 into 7 m × 7 m plots using shovels and tube planters after the ground was rototilled. Planting was conducted at three densities: 196 plants per plot (40,000 plants ha^{-1}, 0.25 m × 0.25 m between rows and within rows spacing; hereafter PD-0.25), 87 plants per plot (17,755 plants ha^{-1}, 0.75 m × 0.75 m; PD-0.75), and 49 plants per plot (10,000 plants ha^{-1}, 1 m × 1 m; PD-1). The typical planting density

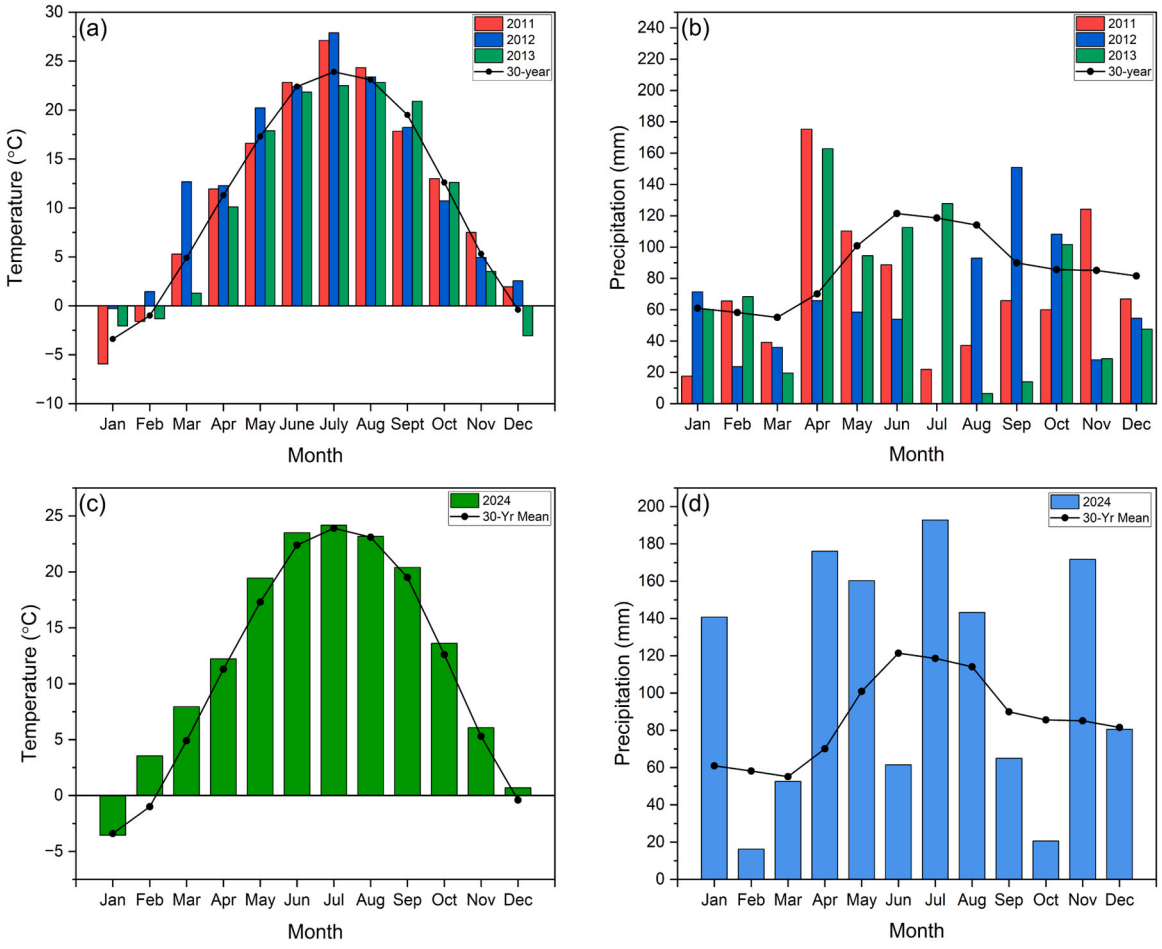

Fig. 2. Mean monthly temperature during 2010–2013 (a) and 2024 (c), and monthly precipitation during 2010–2013 (b) and 2024 (d), along with their 30-year means (1991–2020) at Urbana, IL. Data were obtained from the NOAA, Champaign-Urbana Willard Airport Station, IL.

recommendation for miscanthus is PD-1 (Lee et al., 2018; Lewandowski et al., 2000; Heaton et al., 2008). The densities PD-0.75 and PD-0.25 were chosen to represent the higher-density scenarios. The densities PD-0.75 and PD-0.25 are still logistically practical, as the same or similar densities have been used in several other studies (Namoi et al., 2024; Tejera et al., 2019; Ouattara et al., 2020). Each planting density was achieved with or without 67 kg N ha^{-1} applied as broadcast urea (46−0−0) in early spring from 2011 to 2013, and all plots received 56 kg N ha^{-1} annually from 2014 until 2024. The trial layout was a completely randomized design (CRD) with factorial arrangement of propagule (n = 2) × planting density (n = 3) × N rate (n = 2), resulting in 12 treatment combinations with three replications for a total of 36 experimental units (n = 36). Irrigation and mechanical weed control were provided in 2011 as needed, and plants lost to winterkill or poor establishment were not replaced.

2.2. Data collection and yield measurements

End-of-season biomass yield and yield component traits, including tiller density (tiller m^{-2}), tiller mass (tiller dry mass, g $tiller^{-1}$), and tiller height (cm), were measured during the juvenile and mature phases. The juvenile measurements were taken in the 2011–2013 growing seasons. The mature measurements were taken in the 2024 growing season. Measurements were not taken between 2013 and 2024 due to logistical barriers. Reported biomass yields for the area indicate that 2024 was representative of mature-phase productivity (Figure S2), but the lack of replication is a limitation on mature-phase inferences. All biomass harvest operations occurred from late February to early March following overwintering (post-senescence). Yield-component traits were determined by hand-harvested samples at 10–15 cm stubble height from five random quadrats (1 m × 1 m) within each plot. During 2013, plants from only one plot replicate were hand-harvested for yield-component traits. Consequently, results from 2013 have larger standard errors than results from other years. The biomass from each quadrat was bundled and weighed to obtain fresh matter yield (FM), and individual tillers were counted to estimate tiller density (tillers m^{-2}). Tiller height (cm) was measured from five vegetative and five reproductive tillers. Then, to estimate moisture content, a subsample of ~1.0 kg from each bundle was oven-dried at 60 °C until constant weight. The moisture content was used to adjust FM to dry matter (DM) yield. The mass of individual tillers (g $tiller^{-1}$) was calculated as the bundle dry mass divided by the number of tillers.

After hand sampling, biomass yield in 2012 and 2013 was determined by harvesting the middle ~8.4 m^2 of each plot using a small-plot combine (Wintersteiger Cibus S plot harvester mounted with 1.2-m wide Kemper cutter head, Salt Lake City, UT). During the establishment year (2011), biomass yield was only estimated by hand harvest. Harvesting in 2024 was conducted from the middle ~6.6 m^2 of each plot. The machine-recorded fresh weight for each plot was adjusted to DM using the moisture content estimated from a ~1.0 kg subsample collected from the combine dried at 60 °C until constant mass was achieved.

2.3. Identification of key predictors of miscanthus biomass yield using best-subsets regression

Univariate and multivariate linear regressions were performed to evaluate the relationship between biomass yield and the yield component traits of tiller mass, tiller density, and tiller height. The regressions were evaluated by calculating the coefficient of determination (R^2), root mean square error (RMSE), Akaike Information Criterion corrected (AICc), Bayesian Information Criterion (BIC), and p-value for each linear regression equation. Models were fitted separately by year and propagation method treatment. The best linear regression model was selected from all possible combinations of the independent variables using the best subsets approach. The goodness of fit of the model was evaluated based on AICc. Where models were not significantly different (AICc differences <2), the model with the highest R^2 value was selected (Burnham and Anderson, 2002). In 2013, the regression model including three parameters was excluded because the number of observations was insufficient to support a model with three predictors without overfitting, and the resulting model exhibited unacceptably high AIC values. Therefore, only models supported by the available degrees of freedom and with stable parameter estimates were considered for that year. While the model with the three parameters was excluded in 2013, comparing the goodness of fit of the two-parameter and single-parameter models was sufficient to compare the effect of the yield component traits on the biomass yield.

2.4. Statistical analysis

All data analysis was conducted using JMP Pro 18 (JMP, Cary, NC). Statistical analysis was conducted separately for the juvenile and mature phase data. Treatment effects on biomass yield, tiller mass, tiller density, and tiller height were evaluated using a four-way analysis of variance (ANOVA) for the juvenile phase and three-way ANOVA for the mature phase. For the juvenile phase, planting density (PD), N rate (N), propagation method (P), and year (Y) were included as fixed effects. For mature miscanthus, only PD, N, and P were considered fixed effects. Where differences were significant between treatments ($p \leq 0.05$), Tukey's HSD test was applied for pairwise comparisons.

3. Results

3.1. Juvenile miscanthus: biomass yield and yield components

Biomass yields ranged from 0.4 to 2.3 Mg ha^{-1} in 2011, 6.0–20.5 Mg ha^{-1} in 2012, and 13.4–25.4 Mg ha^{-1} in 2013. The two-way interaction effects Y × PD, P × PD, and Y × N, were significant for juvenile miscanthus biomass yield (Table 1). The biomass yield in the establishment year (2011) was not affected by planting density. In the second year (2012) biomass yields increased with the increased planting density; additionally, biomass yields in 2012 were 5–10 times higher than yields in 2011, depending on planting density. In the third year (2013), there was once again no difference in biomass yields among planting density treatments (Fig. 3a). Within the planting density treatments, biomass yield responded differently between RP and PP methods. For juvenile RP miscanthus, the highest planting density yielded more than the lower planting densities (Fig. 3b). The planting density effects were less obvious in PP miscanthus, as the biomass yield of PD-1 was lower than PD-0.75, but no difference was observed between the yields of PD-0.25

Table 1
Analysis of variance (ANOVA) for the effects of main factors year (Y), propagation method (P), planting density (PD), and nitrogen rate (N), and their interactions, on the end-of-season dry biomass yield and yield component traits of juvenile *Miscanthus* × *giganteus* during growing seasons 2011–2013 at Urbana, IL.

Source of Variance	df	Biomass yield (Mg ha^{-1})	Tiller mass (g $tiller^{-1}$)	Tiller density (tiller m^{-2})	Tiller height (cm)
Year (Y)	1	< 0.0001	< 0.0001	< 0.0001	< 0.0001
Propagule (P)	1	0.0205	< 0.0001	< 0.0001	< 0.0001
Planting Density (PD)	2	0.0003	< 0.0001	0.3907	0.0016
N Rate (N)	1	0.0005	0.0253	0.3377	0.1946
Y × P	1	0.1793	0.0002	0.0151	0.023
Y × PD	2	< 0.0001	< 0.0001	0.0007	< 0.0001
Y × N	1	0.0114	0.0608	0.4947	0.1696
P × PD	2	0.0091	0.0008	0.7688	0.0274
P × N	1	0.0627	0.8895	0.7763	0.7627
PD x N	2	0.6910	0.0746	0.6341	0.2058
Y × P × PD	2	0.5645	0.2517	0.5461	0.2189
Y × P × N	1	0.1665	0.3004	0.5477	0.9708
Y × PD x N	2	0.9626	0.0201	0.700	0.6234
P × PD x N	2	0.4046	0.0131	0.6493	0.6096
Y × P x PD x N	2	0.3510	0.0126	0.866	0.1439

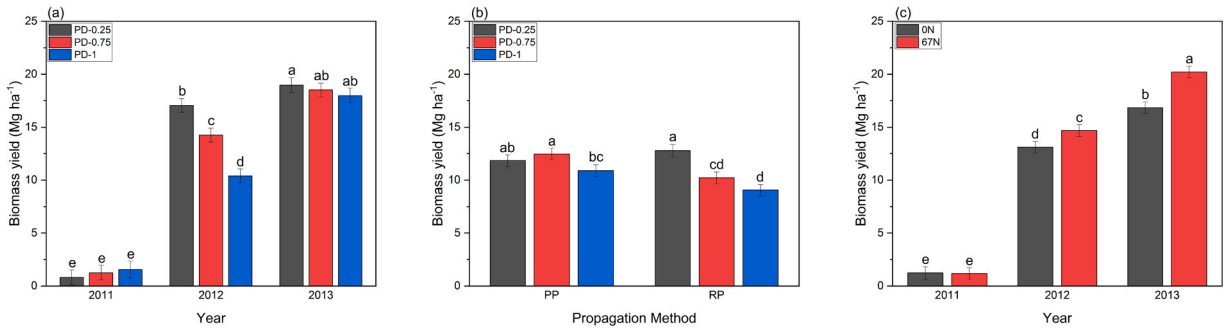

Fig. 3. Mean annual dry biomass yield (Mg ha^{-1}) of juvenile *Miscanthus* × *giganteus* affected by (a) the interaction of year and planting density (0.25 m^2, 0.75 m^2, and 1 m^2 between plants), (b) the interaction of propagation method (PP = plug, RP = rhizome) and planting density, and (c) the interaction of year and N fertilization (0 and 67 kg N ha^{-1}) during growing seasons 2011, 2012, and 2013 at Urbana, IL. Letters above bars indicate mean comparisons; bars sharing the same letter are not significantly different at $p < 0.05$. Error bars indicate the standard errors of the differences of means.

and PD-0.75 (Fig. 3b). Comparing the propagation methods, RP and PP yielded similarly when planted at high planting density (PD-0.25) (Fig. 3b). At the lower planting densities, especially PD-1, RP miscanthus yielded less than PP miscanthus (Fig. 3b). Applying N increased the average yield by 1.6 Mg ha^{-1} (12 %) in 2012 and by 3.4 Mg ha^{-1} (21 %) in 2013, but did not significantly affect yield in 2011 (Fig. 3c).

Miscanthus tiller mass increased as the stands got older (Fig. 4a), and the rate of increase was affected by propagation methods, planting density, and their interaction during the juvenile phase (Table 1). The interaction effect of propagation methods and year showed that higher tiller mass was achieved by RP miscanthus than PP miscanthus; on average, RP tillers were 3.3 g tiller^{-1} heavier in 2011, 6.3 g tiller^{-1} heavier in 2012, and 6.4 g tiller^{-1} heavier in 2013 (Fig. 4a). Tiller mass in 2012 was greatest for the PD-0.25, but in 2013 the PD-1 produced the heaviest tillers on average (Fig. 4b). Planting density also interacted with propagation method to affect tiller mass. High planting density produced heavier tillers for RP miscanthus, but in PP miscanthus no difference between planting densities was observed (Fig. 4c).

Tiller density in juvenile miscanthus was affected by the two-way interactions Y × P and Y × PD (Table 1). Tiller density increased from 2011 to 2012, and the PP miscanthus produced more tillers on average than RP (Fig. 5a). Tiller density for PP miscanthus was 62 % greater than RP in 2011, then only 31 % greater in 2012, and finally 16 % greater in 2013. Between levels of planting density, PD-0.25 had the lowest tiller density in 2011 (Fig. 5b). In 2012, PD-0.25 tiller density was similar to PD-0.75, and PD-1 produced the lowest tiller density. In 2013 the miscanthus stands were transitioning to, or had achieved, canopy density equilibrium. As a result, tiller density was not significantly different between the propagation methods (Fig. 5a) or the planting densities (Fig. 5b).

Similar to tiller mass, the tiller height of juvenile miscanthus was influenced by the interactions between year and propagation method (Y × P) and between year and planting density (Y × PD) (Table 1). Tiller height increased between years (Fig. 6a). A significant effect of planting density on tiller height was detected only in 2012, when higher planting densities produced taller tillers (Fig. 6a). Generally, RP miscanthus exhibited greater tiller height than PP miscanthus (Figs. 6b). On average, the RP miscanthus produced taller tillers at the highest planting density, while no difference was detected for PP miscanthus between planting densities (Fig. 6c). The results in Fig. 6c are similar to the observed effect on tiller mass by the interaction between propagation method and planting density (Fig. 6c), likely due to a positive correlation between tiller height and tiller mass (Lim et al., 2021).

3.2. Mature miscanthus: biomass yield and yield components

The mean biomass yield of mature miscanthus in 2024 was 14.5 Mg ha^{-1} . The mature-phase measurements were discontinuous with an eleven-year gap from the 2013 juvenile-phase measurements. While this limits the strength of interpretation, biomass yield data for the area indicate that 2024 was representative of the mature-phase productivity (Figure S2). In 2024, biomass yield was lower than the third-year mean of 18.5 Mg ha^{-1} (2013) but similar to the second-year mean of 13.9 Mg ha^{-1} (2012) (Figure S2b). Propagation method and planting density had no significant effect on mature-phase yields in 2024 (Table 2). The yields observed in this study are comparable to machine-harvested values reported for similarly aged stands in the Midwest (10–17 Mg ha^{-1} (Sharma et al., 2022; Namoi et al., 2024, 2022). Although no yield data were collected from 2014 to 2023, records from the surrounding field area indicate that maximum productivity was reached in 2013 and

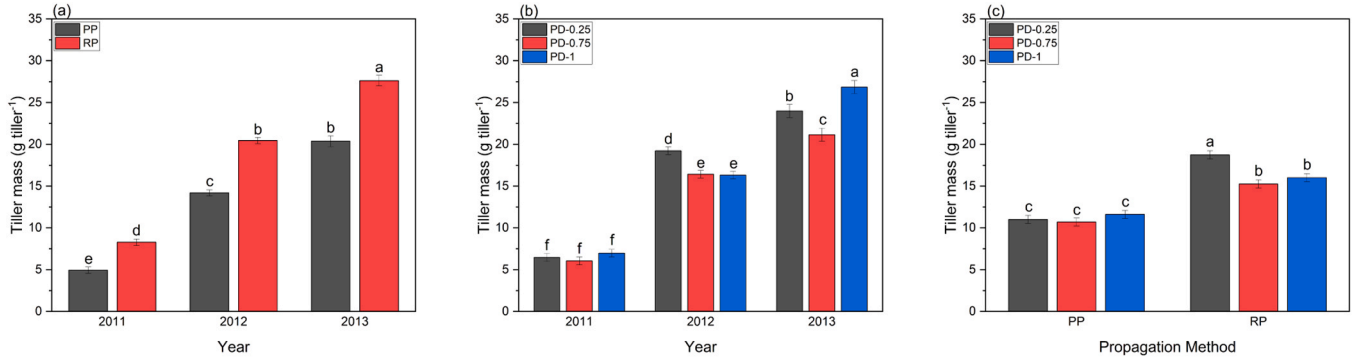

Fig. 4. Mean annual tiller mass (g tiller^{-1}) of juvenile *Miscanthus* × *giganteus* stands affected by (a) the interaction of year and propagation method (PP = plug, RP = rhizome), (b) the interaction of year and planting density (0.25 m^2, 0.75 m^2, and 1 m^2 between plants), and (c) the interaction of propagation method and planting density. Letters above bars indicate mean comparisons; bars sharing the same letter are not significantly different at $p < 0.05$. Error bars indicate the standard errors of the differences of means.

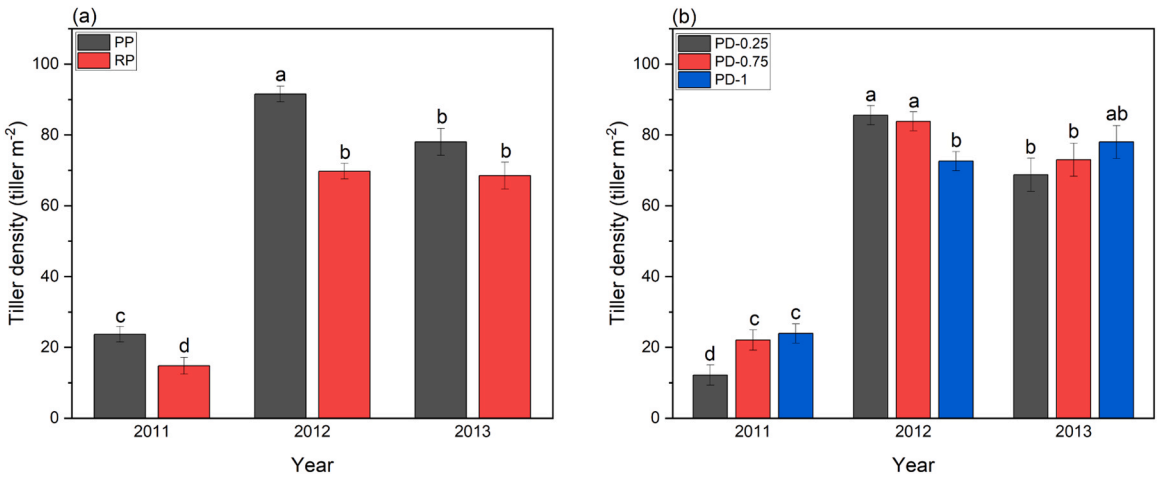

Fig. 5. Mean annual tiller density (tiller m^{-2}) of juvenile *Miscanthus* × *giganteus* stands affected by (a) interaction of year and propagation method (PP = plug, RP = rhizome), and (b) the interaction of year and planting density (0.25 m^2, 0.75 m^2 and 1 m^2 between plants). Letters above bars indicate mean comparisons; bars sharing the same letter are not significantly different at $p < 0.05$. Error bars indicate the standard errors of the differences of means.

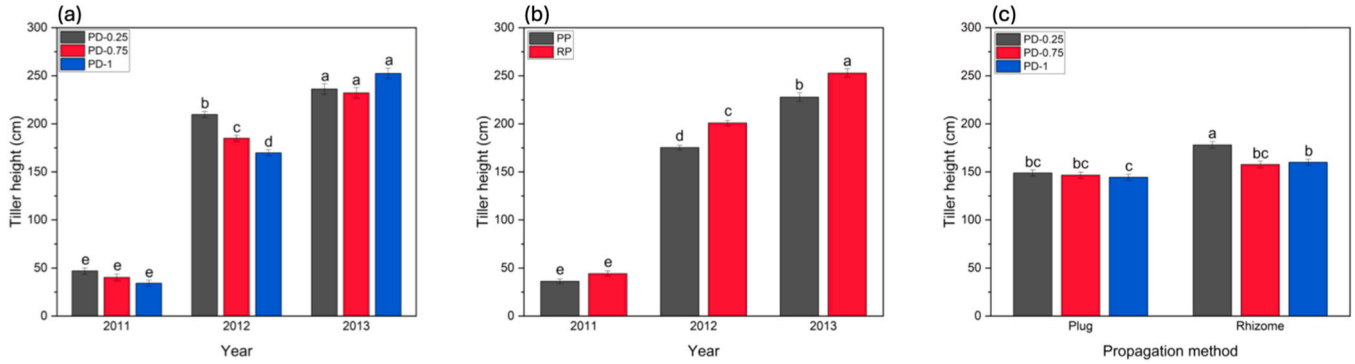

Fig. 6. Mean annual tiller height (cm) of juvenile *Miscanthus* × *giganteus* stands affected by (a) the interaction of year and planting density (0.25 m^2, 0.75 m^2, and 1 m^2 between plants), (b) the interaction of year and propagation method (PP = plug, RP = rhizome), and (c) the interaction of propagation method and planting density. Letters above bars indicate mean comparisons; bars sharing the same letter are not significantly different at $p < 0.05$. Error bars indicate the standard errors of the differences of means.

Table 2
Analysis of variance (ANOVA) for the effects of main factors propagation method (P), planting density (PD), and nitrogen rate (N), and their interactions, on the end-of-season dry biomass yield and yield component traits of mature (~14-year-old) *Miscanthus* × *giganteus* during the growing season 2024 at Urbana, IL.

Source of variance	df	Biomass yield (Mg ha^{-1})	Tiller mass (g $tiller^{-1}$)	Tiller density (tiller m^{-2})	Tiller height (cm)
Propagule (P)	1	0.5227	0.0008	0.0013	< 0.0001
Planting Density (PD)	2	0.0577	0.2980	0.3761	0.1597
N Rate (N)	1	0.6467	0.4022	0.7920	0.2941
P × PD	2	0.1557	0.4026	0.1299	0.7182
P × N	1	0.8146	0.2504	0.3867	0.2837
N × PD	2	0.8913	0.6827	0.5066	0.5376
P × N × PD	2	0.4618	0.4843	0.7282	0.6834

subsequently stabilized at an average of 12.2 Mg ha^{-1} (Figure S2). This pattern confirms that the effects of planting density and propagation method on biomass yield diminished as stands matured, and ultimately disappeared by 2024 (Table 2).

The propagation method was a significant main effect on all three yield components. The mean tiller mass for mature RP miscanthus was 46.1 g $tiller^{-1}$, which was 30 % heavier than the mean tiller mass of PP miscanthus (Fig. 7a). In contrast, the mean tiller density for RP miscanthus was 55 tillers m^{-2}, which was 15 % less than the mean tiller density of PP miscanthus (Fig. 7b). The mean RP miscanthus tiller height was 344 cm, which was 10 % taller than the mean PP miscanthus tiller height (Fig. 7c).

3.3. Yield component changes through growth phases

Univariate and multivariate linear regression revealed the relative contribution of each yield component to variation in biomass yield (Table 3). Due to the consistent morphological difference between propagation methods (Figs. 4a, 5a, and 6b), separate regressions were performed for PP miscanthus and RP miscanthus. In 2011 and 2012, the tiller density had the strongest univariate relationship with biomass yield. The exception to this was RP miscanthus in 2012, where tiller height had a stronger relationship to yield, while tiller density and tiller mass had similar performance in univariate regressions. In 2013, both propagation methods had the strongest univariate relationship between tiller mass and yield. For mature miscanthus in 2024, tiller density no longer had a significant relationship with the final yield. For 2024 PP miscanthus, the univariate relationships between yield and tiller mass or tiller height were similar (Lim et al., 2021; Robson et al., 2013). For 2024 RP miscanthus, tiller mass had a stronger univariate performance.

In the multivariate regressions, models that contained both tiller

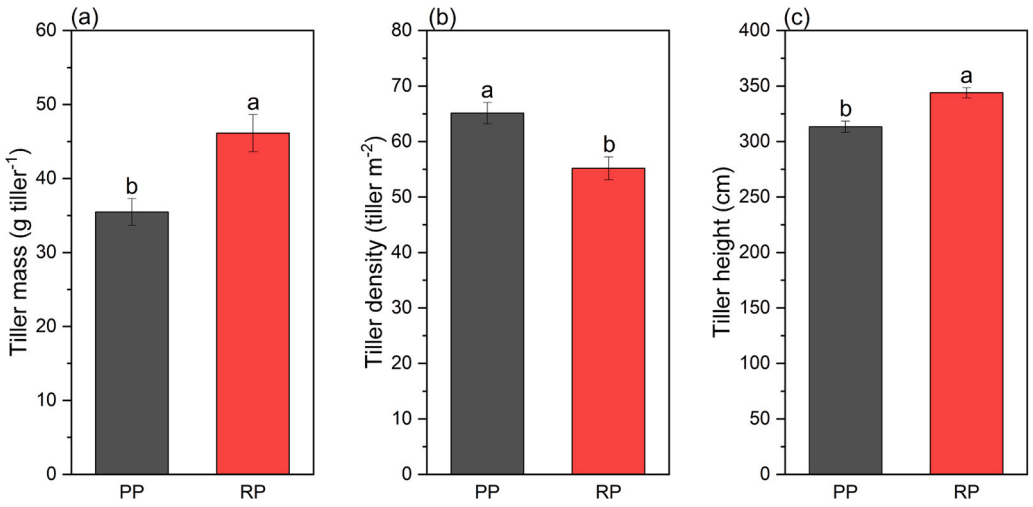

Fig. 7. Effect of propagation method (PP = plug, RP = rhizome) on (a) tiller mass (g tiller^{-1}), (b) tiller density (tillers m^{-2}), and (c) tiller height (cm) in mature *Miscanthus* × *giganteus* stands in Urbana, IL. Letters above bars indicate mean comparisons; bars sharing the same letter are not significantly different at $p < 0.05$. Error bars indicate the standard errors of the differences of means.

density and tiller mass generally had stronger relationships to biomass yield (Table 3). Including tiller height generally had a negligible impact on model performance metrics. In 2024 for RP miscanthus, including tiller height minorly improved the multivariate regression's R^2 and RMSE values, despite the univariate relationship between tiller height and yield being weaker in 2024 RP miscanthus than in 2024 PP miscanthus.

4. Discussion

4.1. Nitrogen fertilization timing influences yield recovery between juvenile and mature miscanthus phases

Previous studies have shown that Nitrogen (N) application may increase miscanthus tiller mass by approximately 55 %–71 % (Lee et al., 2017; Namoi et al., 2024). Our juvenile phase results suggested a weaker N response, as observed by the 12 % increase in yield in 2012 and the 21 % increase in 2013 (Fig. 3c). The effect of N application on the mature phase miscanthus was likely confounded in our study by the uniform annual fertilization (56 kg N ha^{-1}) applied to all plots starting in 2014. Thus, the mature miscanthus data essentially compared yields in plots that began fertilizer application during establishment (67 kg N ha^{-1} starting in 2011) to yields in plots that began application after establishment (56 kg N ha^{-1} starting in 2014). Our results suggest that when low yields in the juvenile phase can be attributed to N limitations, late initiation of a fertilizer regime may enable yield recovery. In other words, neglecting to fertilize miscanthus during the juvenile phase may not permanently lower yield potential for subsequent years. Yield recovery following resumed N fertilization has been observed by other groups (Anderson et al., 2011; Namoi et al., 2024; Kantola et al., 2022). However, whether the maximum yield potential can be fully restored remains uncertain, considering the environmental complexity and seasonal changeability that contribute to N response in yield and yield component traits (Anderson et al., 2011; Namoi et al., 2024).

4.2. Stand age and planting density regulate the shift from density-driven to mass-driven yield formation

Perennial stand age (represented by year) influences the tiller density at both the canopy and individual plant level (Figs. 5a, 5b). During the juvenile yield-building phase, tiller density showed the strongest univariate relationship with yield, because the miscanthus canopy was still developing (Table 3, Figure S1). Miscanthus has a rhizomatous growth habit that enables it to fill empty space between plants relatively quickly (Tejera et al., 2021; Arundale et al., 2014), whether those gaps result from intentional planting skips or failed establishment. Consequently, tiller density has a strong relationship with biomass yield during this phase (Table 3). Once rhizomatous growth fills the canopy gaps, the canopy density becomes limited by competition among neighboring plants for space, light, and nutrients. Competition for resources causes plant to regulate their vegetative growth, which is conducted through control of hormonal gene expression (Zhou et al., 2025, 2023; Yang and Li, 2017; Liu et al., 2023; He et al., 2023). The change from expanding tiller density to internally-regulated tiller density is an indication that the miscanthus stand has established a canopy density equilibrium (Fig. 1) (Namoi et al., 2026). From this point onward, the biomass yield is more strongly related to tiller mass (Table 3). The potential tiller mass is constrained in part by the established canopy density equilibrium, because tiller density and tiller thickness have an inverse relationship. Lower tiller density enables individual plants to support greater tiller thicknesses, and vice versa (Namoi et al., 2024; Njuguna et al., 2023). Therefore, once the stand reaches canopy density equilibrium, yield is determined by the maximum tiller mass attainable within the given canopy density.

Planting density was observed to influence the rate at which the canopy density equilibrium was achieved, in relation to maximum productivity. Previous literature suggests that while planting density does not dictate yield potential, the planting density does affect how many years are required for the perennial stand to potentially achieve maximum productivity (Lewandowski et al., 2000; Miguez et al., 2008). The meta-analysis by Miguez et al (Miguez et al., 2008). identified the second growing season as most affected by plant density. This aligns with our results, which showed a higher biomass yield at higher planting density for both PP miscanthus and RP miscanthus in 2012, followed by marginal differences between planting densities in 2013, and no differences in 2024 (Fig. 3a). Higher planting density encouraged greater tiller density, which supported higher yields sooner in the density-dominated juvenile phase (Table 3). Over time, however, all planting densities achieved similar yields (Table 2), again supporting the conclusion that planting density affects how quickly a stand reaches maximum productivity but does not change the maximum productivity potential.

Table 3
Summary of univariate and multivariate linear regressions between *Miscanthus* × *giganteus* biomass yield (Y, Mg ha^{-1}) and tiller density (D, tiller m^{-2}), tiller mass (M, g tiller^{-1}), and tiller height (H, cm). Separate regressions were performed by propagation method, either plug (PP) or rhizome (RP).

Year	Propagule	Model	Parameter(s)	Model Equation	R^2	RMSE	AICc	BIC	p-value
2011	PP	1	Density, Mass	Y = -1.232 + 0.048*D + 0.261*M	0.975	0.098	-24.9	-24.4	< 0.0001
		2	Density, Mass, Height	Y = -1.147 + 0.003*D + 0.024*M – 0.167*H	0.976	0.099	-21.8	-24.9	< 0.0001
		3	Density	Y = -0.186 + 0.059*D	0.778	0.283	11.2	12.2	< 0.0001
		4	Density, Height	Y = -0.011 + 0.057*D – 0.374*H	0.783	0.289	14.1	14.6	< 0.0001
		5	Mass	Y = -0.737 + 0.395*M	0.504	0.423	25.7	26.6	0.0010
		6	Mass, Height	Y = -0.18 + 0.368*M	0.561	0.411	26.8	27.3	0.0021
		7	Height	Y = 1.852 – 1.805*H	0.138	0.557	35.6	36.6	0.1287
	RP	1	Density, Mass	Y = -1.002 + 0.077*D + 0.129*M	0.973	0.051	-41.2	-41.8	< 0.0001
		2	Density, Mass, Height	Y = -0.797 + 0.076*D + 0.135*M – 0.129*H	0.975	0.052	-37.9	-40.1	< 0.0001
		3	Density, Height	Y = -0.382 + 0.080*D + 0.866*H	0.673	0.181	-1.0	-1.6	0.0007
		4	Density	Y = 0.125 + 0.073*D	0.553	0.204	0.4	0.7	0.0010
		5	Mass	Y = 0.218 + 0.119*M	0.466	0.244	6.1	6.4	0.0142
		6	Mass, Height	Y = 0.255 + 0.151*M – 0.674*H	0.409	0.243	8.5	7.9	0.0326
		7	Height	Y = 1.016 + 0.409*H	0.028	0.300	12.8	13.1	0.5333
2012	PP	1	Density, Mass	Y = -8.541 + 0.132*D + 0.675*M	0.954	0.472	31.8	32.3	< 0.0001
		2	Density, Mass, Height	Y = -0.872 + 0.129*D + 0.664*M + 0.315*H	0.954	0.487	35.6	35.1	< 0.0001
		3	Density, Height	Y = -2.678 + 0.083*D + 4.672*H	0.726	1.150	63.9	64.4	< 0.0001
		4	Density	Y = 2.786 + 0.113*D	0.645	1.269	65.2	66.2	0.0001
		5	Height	Y = -3.199 + 9.284*H	0.504	1.498	71.2	72.2	0.0010
		6	Mass, Height	Y = -5.382 + 0.229*M + 8.680*H	0.539	0.478	73.2	73.7	0.0030
		7	Mass	Y = 7.263 + 0.415*M	0.124	1.990	81.5	82.4	0.1521
	RP	1	Density, Mass	Y = -14.416 + 0.203*D + 0.725*M	0.991	0.305	16.2	16.6	< 0.0001
		2	Density, Mass, Height	Y = -14.445 + 0.217*D + 0.849*M – 1.742*H	0.992	0.290	17.0	16.5	< 0.0001
		3	Density, Height	Y = -12.641 + 0.129*D + 9.069*H	0.929	0.834	52.3	52.8	< 0.0001
		4	Height	Y = -7.853 + 11.179*H	0.749	1.523	71.8	72.8	< 0.0001
		5	Mass, Height	Y = -8.449 – 0.349*M + 15.035*H	0.774	1.493	73.3	73.8	< 0.0001
		6	Density	Y = 0.533 + 0.201*D	0.500	2.152	84.3	85.2	0.0010
		7	Mass	Y = -0.118 + 0.718*M	0.481	2.192	84.9	85.9	0.0014
2013	PP	1	Density, Mass	Y = -13.902 + 0.177*D + 0.790*M	0.997	0.244	43.9	3.1	0.0001
		2	Mass, Height	Y = -16.473 + 0.803*M + 7.035*H	0.964	0.916	59.8	19.0	0.0070
		3	Mass	Y = -7.693 + 1.161*M	0.947	0.956	32.0	19.4	0.0011
		4	Height	Y = -30.615 + 20.393*H	0.893	1.357	36.3	23.6	0.0044
		5	Density, Height	Y = -28.489 + 0.164*D + 13.398*H	0.916	1.388	64.8	24.0	0.0242
		6	Density	Y = -17.092 + 0.424*D	0.847	1.624	38.4	25.8	0.0092
	RP	1	Density, Mass	Y = -19.668 + 0.294*D + 0.669*M	0.987	0.553	53.8	12.9	0.0013
		2	Density, Height	Y = -55.173 + 0.351*D + 20.039*H	0.968	0.895	59.5	18.7	0.0056
		3	Mass, Height	Y = 9.694 + 0.936*M – 6.628*H	0.804	2.229	70.5	29.7	0.0869
		4	Mass	Y = -1.188 + 0.730*M	0.798	1.959	40.7	28.0	0.0165
		5	Height	Y = -33.308 + 20.917*H	0.691	2.422	43.2	30.6	0.0403
		6	Density	Y = -7.478 + 0.386*D	0.337	3.549	47.8	35.2	0.2271
2024	PP	1	Density, Mass	Y = -17.714 + 0.297*D + 0.465*M	0.985	0.505	34.3	34.8	< 0.0001
		2	Density, Mass, Height	Y = -18.719 + 0.289*D + 0.451*M + 0.641*H	0.986	0.516	37.7	37.2	< 0.0001
		3	Mass, Height	Y = -20.395 + 0.202*M + 10.018*H	0.770	2.004	83.9	84.4	< 0.0001
		4	Height	Y = -29.168 + 15.101*H	0.691	2.250	85.9	86.8	< 0.0001
		5	Density, Height	Y = -32.377 + 0.101*D + 14.018*H	0.733	2.164	86.7	87.1	< 0.0001
		6	Mass	Y = 3.981 + 0.399*M	0.618	2.501	89.7	90.7	0.0001
		7	Density	Y = 4.749 + 0.206*D	0.184	3.659	103.4	104.3	0.0755
	RP	1	Density, Mass	Y = -19.450 + 0.340*D + 0.442*M	0.955	0.877	54.2	54.6	< 0.0001
		2	Density, Mass, Height	Y = -25.764 + 0.340*D + 0.416*M + 2.187*H	0.962	0.837	55.1	54.6	< 0.0001
		3	Mass	Y = 6.844 + 0.278*M	0.575	2.621	91.4	92.3	0.0003
		4	Mass, Height	Y = 0.582 + 0.252*M + 2.170*H	0.582	2.686	94.4	94.9	0.0015
		5	Height	Y = -19.075 + 11.269*H	0.314	3.330	100.0	100.9	0.0156
		6	Density, Height	Y = -35.529 + 0.143*D + 13.755*H	0.401	3.213	100.9	101.4	< 0.0213
		7	Density	Y = 18.287 + 0.025*D	0.003	4.014	106.7	107.7	0.3203

4.3. Morphological tradeoffs and survival dynamics between rhizome- and plug-propagated miscanthus

Across all planting densities, we observed that tiller density and tiller mass measurements were different between the propagation methods, rhizome (RP) and plug (PP). Tiller density was higher in PP plots in 2011, 2012, and 2013 (Fig. 5a). However, tiller mass was greater in RP plots in 2011, 2012, and 2013 (Fig. 5b). This tradeoff between tiller density and mass can be observed in Figure S3. These findings agree with previous reports that RP miscanthus produces fewer and larger tillers (Namoi et al., 2024; Lewandowski et al., 2000; Boersma and Heaton, 2014b; Njuguna et al., 2023). Based on the relationships between yield, tiller density, and tiller mass (Table 3), the higher tiller density in PP plots produced higher yields during the juvenile phase. Additionally, the PP plots could achieve the previously discussed canopy density equilibrium sooner than the RP plots. The exception to this trend was the highest planting density (PD-0.25), which had similar yields between RP and PP, possibly attributable to the PD-0.25 creating an artificially higher tiller density across the total harvesting area. However, as plots established their canopy density equilibria, RP miscanthus closed the yield gap by achieving higher tiller mass that compensated for lower tiller density. The morphological difference between RP and PP plants was still observable in 2024 (Figs. 7a and 7b), but the propagule-determined tradeoff between tiller density and mass had closed the yield gap between RP and PP plots (Table 2).

Another notable observation was the rates of survival between RP and PP at different planting densities. Survival rate is another component contributing to the end-of-season biomass yield. Survival rate data were not measured during the growing season, but a satellite image of the 2012 growing season enabled a retroactive estimate of plot

population (Figure S1). Based on this rough estimation, PP plots had a higher rate of survival than RP plots. At the lowest planting density (PD-1.0), the PP plots had a mean rate of 87 % survival, compared to RP plots at 67 % survival (Figure S1). At the moderate planting density (PD-0.75), PP plots had a 78 % survival rate compared to RP plots at 61 % survival. The survival rates could not be reliably estimated at the highest planting density (PD-0.25). The PP plants may have had an advantage due to their well-developed root system prior to transplant, compared to rhizomes which possess few or no roots at transplant (Arundale et al., 2014). These observations may suggest that planting density and propagation method both contribute to survival rate in the early juvenile phase. Ground-truthing data from multiple years would be needed to verify this proposed hypothesis. Additionally, it is unclear if the higher survival rates would justify the greater establishment costs associated with high planting density, especially considering that the yield gap between planting densities diminished by 2013 (Fig. 3a) and disappeared in the mature stand in 2024 (Table 2).

The different survival rates of RP and PP may contribute to the morphological tradeoff between the two propagation methods. The higher survival rate of PP may have led to more tillers per area, causing a shading effect that reduced light interception. The increased competition for light could have altered the physiology of tiller growth. This has been observed in cotton, where closely spaced plants exhibit stronger apical dominance, resulting in reduced branching and stronger upper canopy growth (Zhou et al., 2025, 2023). This change in physiology was driven by down-regulating genes responsible for auxin (IAA), cytokinin (CK), and gibberellin (GA) production, which was triggered by reduced red/far-red ratio and photosynthetically active radiation (Zhou et al., 2025, 2023). This phenomenon is not limited to cotton and has been observed in other crop species (Yang and Li, 2017; Liu et al., 2023; He et al., 2023). Likewise, PP miscanthus may be experiencing reduced space between tillers, which causes hormonal regulation to reduce resource allocation per tiller, finally resulting in reduced tiller mass compared to RP miscanthus. Boersma and Heaton (Boersma and Heaton, 2014a) also proposed that the morphological difference between RP and PP is caused by intrinsic properties of the aerial organs, including their native hormonal profiles. However, to our knowledge, no research has yet revealed the relationship between hormonal gene expression and tiller morphology of miscanthus. Therefore, further research is required to determine how propagation method–specific differences in hormonal gene expression drive variation in tiller morphology.

4.4. Principal implications of establishment and management practices for miscanthus productivity

Our results show that establishment methods—planting density, propagation method, and N fertilization—strongly affected biomass yield and yield components during the juvenile phase. The influence of establishment methods had little influence on the mature stands, though this observation is weakened by the aforementioned gap in observations between 2013 and 2024. The early yield advantage of plug-propagated miscanthus resulted from faster canopy development, but this difference declined as rhizome-propagated plants developed heavier tillers and achieved yield parity (Fig. 1). The shift from tiller density to tiller mass as the strongest univariate relationship to yield reflects a developmental change in resource allocation. Therefore, management should prioritize rapid establishment through adequate planting density and appropriate propagation choice during the early years, whereas long-term yield stability depends mainly on maintaining tiller mass. Overall, while establishment practices determine early growth and canopy formation, mature-phase productivity is ultimately governed by miscanthus's intrinsic capacity to balance tiller density and mass.

5. Conclusion

Sustainable miscanthus cultivation requires understanding how propagation method, planting density, and N management support productivity. Linear regression models identified the relative weights of tiller density, tiller mass, and tiller height on end-of-season biomass yield. All three tiller component traits contribute to biomass yield, but tiller density was the strongest predictor during the early juvenile phase. After canopy density equilibrium was established, tiller mass replaced tiller density as the strongest predictor. The RP miscanthus had lower tiller density than PP miscanthus, giving PP plots a yield advantage in the early juvenile phase. Higher tiller density also enabled PP miscanthus to achieve canopy density equilibrium sooner. The RP miscanthus had lower tiller density, but greater tiller mass and tiller height than PP miscanthus. Thus, after RP reached canopy density equilibrium, the RP plots attained yields similar to the PP miscanthus. The compensatory tradeoff between tiller mass and density was also observed in mature miscanthus. Planting density also affected juvenile phase biomass yield. Higher planting density produced greater yields in the early juvenile phase, and accelerated canopy equilibrizing for both RP and PP plots. Nitrogen application provided only a modest increase in juvenile phase yields. Fertilizer application from 2014 to 2024 masked any observable difference in biomass yield between fertilized and unfertilized mature miscanthus. This suggests that N deficiency in the juvenile phase may not limit mature phase productivity if fertilization is resumed or initiated later. Overall, higher planting density, the PP method, and N fertilizer were observed to accelerate canopy density equilibrizing, which resulted in higher juvenile phase yields. However, the yield gains diminished after the stands achieved canopy density equilibrium. An economic analysis is needed to determine whether the higher productivity in the early juvenile years can justify the higher establishment cost of methods that accelerate canopy density equilibrizing.

CRediT authorship contribution statement

DoKyoung Lee: Writing – review & editing, Supervision, Project administration, Funding acquisition, Conceptualization. **Jung Woo Lee:** Writing – original draft, Investigation, Formal analysis, Data curation, Conceptualization. **Vittore Kayla:** Writing – original draft, Investigation, Formal analysis, Data curation, Conceptualization. **Nictor Namoi:** Writing – review & editing, Formal analysis. **Soonho Hwang:** Writing – review & editing.

Declaration of Generative AI and AI-assisted technologies in the writing process

During the preparation of this work, the author(s) used ChatGPT 5 for editing. After using this tool/service, the author(s) reviewed and edited the content as needed and take(s) full responsibility for the content of the published article.

Declaration of Competing Interest

The authors have no relevant financial or non-financial interests to disclose.

Acknowledgments

This work was funded by the DOE Center for Advanced Bioenergy and Bioproducts Innovation (U.S. Department of Energy, Office of Science, Biological and Environmental Research Program under Award Number DE-SC0018420). Any opinions, findings, and conclusions or recommendations expressed in this publication are those of the author (s) and do not necessarily reflect the views of the U.S. Department of Energy.

Appendix A. Supporting information

Supplementary data associated with this article can be found in the online version at doi:10.1016/j.indcrop.2025.122611.

Data availability

Data will be made available on request.

References

Anderson, E., Arundale, R., Maughan, M., Oladeinde, A., Wycislo, A., Voigt, T., 2011. Growth and agronomy of *Miscanthus* x *giganteus* for biomass production. Biofuels 2, 71–87. https://doi.org/10.4155/bfs.10.80.

Arundale, R.A., Dohleman, F.G., Voigt, T.B., Long, S.P., 2014. Nitrogen fertilization does significantly increase yields of stands of miscanthus × giganteus and panicum virgatum in multiyear trials in illinois. Bioenerg. Res. 7, 408–416. https://doi.org/10.1007/s12155-013-9385-5.

Aslan-Sungur (Rojda), G., Boersma, N., Moore, C.E., Heaton, E., Bernacchi, C.J., Vanloocke, A., 2025. Advances in Miscanthus × Giganteus planting techniques may increase carbon uptake in the establishment year. GCB Bioenergy 17, e70012. https://doi.org/10.1111/gcbb.70012.

Assefa, Y., Vara Prasad, P.V., Carter, P., Hinds, M., Bhalla, G., Schon, R., Jeschke, M., Paszkiewicz, S., Ciampitti, I.A., 2016. Yield responses to planting density for us modern corn hybrids: a synthesis-analysis. Crop Sci. 56, 2802–2817. https://doi.org/10.2135/cropsci2016.04.0215.

Atkinson, C.J., 2009. Establishing perennial grass energy crops in the UK: A review of current propagation options for Miscanthus. Biomass.. Bioenergy 33, 752–759. https://doi.org/10.1016/j.biombioe.2009.01.005.

Boersma, N.N., Heaton, E.A., 2012. Effects of temperature, illumination and node position on stem propagation of *Miscanthus* × *giganteus*. Glob. Change Biol. Bioenergy 4, 680–687. https://doi.org/10.1111/j.1757-1707.2011.01148.

Boersma, N.N., Heaton, E.A., 2014a. Propagation method affects Miscanthus×giganteus developmental morphology. Ind. Crops Prod. 57, 59–68. https://doi.org/10.1016/j.indcrop.2014.01.059.

Boersma, N.N., Heaton, E.A., 2014b. Does propagation method affect yield and survival? The potential of Miscanthus×giganteus in Iowa, USA. Ind. Crops Prod. 57, 43–51. https://doi.org/10.1016/j.indcrop.2014.01.058.

Burnham, K.P., Anderson, D.R., 2002. Model Selection and Multimodel Inference: A Practical Information-Theoretic Approach, 2nd ed. Springer New York, NY, USA. https://doi.org/10.1007/b97636.

Cadoux, S., Riche, A.B., Yates, N.E., Machet, J.-M., 2012. Nutrient requirements of Miscanthus x giganteus: Conclusions from a review of published studies. Biomass.. Bioenergy 38, 14–22. https://doi.org/10.1016/j.biombioe.2011.01.015.

Chae, W.B., Hong, S.J., Gifford, J.M., Lane Rayburn, A., Widholm, J.M., Juvik, J.A., 2013. Synthetic polyploid production of Miscanthus sacchariflorus, Miscanthus sinensis, and Miscanthus x giganteus. GCB Bioenergy 5, 338–350. https://doi.org/10.1111/j.1757-1707.2012.01206.x.

Christian, D.G., Riche, A.B., Yates, N.E., 2008. Growth, yield and mineral content of *Miscanthus* × *giganteus* grown as a biofuel for 14 successive harvests. Ind. Crops Prod. 28, 320–327. https://doi.org/10.1016/j.indcrop.2008.02.009.

Clifton-Brown, J.C., Lewandowski, I., 2002. Screening *Miscanthus* genotypes in field trials to optimise biomass yield and quality in Southern Germany. Eur. J. Agron. 16, 97–110. https://doi.org/10.1016/S1161-0301(01)00120-4.

Dalton, S., 2013. Biotechnology of Neglected and Underutilized Crops, in: ResearchGate, 2013. https://doi.org/10.1007/978-94-007-5500-0_11.

Danalatos, N., Archontoulis, S., Mitsios, I., 2007. Potential growth and biomass productivity of Miscanthus×giganteus as affected by plant density and N-fertilization in central Greece. Biomass. Bioenergy 31, 145–152. https://doi.org/10.1016/j.biombioe.2006.07.004.

Dohleman, F.G., Long, S.P., 2009. More productive than maize in the midwest: how does miscanthus do it? Plant Physiol. 150, 2104–2115. https://doi.org/10.1104/pp.109.139162.

He, L., Xu, M., Wang, W., Liu, C., Yu, L., Liu, W., Yang, W., 2023. The interaction between strigolactone and auxin results in the negative effect of shading on soybean branching development. Agronomy 13, 2383. https://doi.org/10.3390/agronomy13092383.

Heaton, E.A., Dohleman, F.G., Long, S.P., 2008. Meeting US biofuel goals with less land: the potential of Miscanthus. Glob. Change Biol. 14, 2000–2014. https://doi.org/10.1111/j.1365-2486.2008.01662.x.

Kane, J.L., Schartiger, R.G., Daniels, N.K., Freedman, Z.B., McDonald, L.M., Skousen, J. G., Morrissey, E.M., 2023. Bioenergy crop Miscanthus x giganteus acts as an ecosystem engineer to increase bacterial diversity and soil organic matter on marginal land. Soil Biol. Biochem. 186, 109178. https://doi.org/10.1016/j.soilbio.2023.109178.

Kantola, I.B., Masters, M.D., Blanc-Betes, E., Gomez-Casanovas, N., DeLucia, E.H., 2022. Long-term yields in annual and perennial bioenergy crops in the Midwestern United States. GCB Bioenergy 14, 694–706. https://doi.org/10.1111/gcbb.12940.

Lee, D.K., Aberle, E., Anderson, E.K., Anderson, W., Baldwin, B.S., Baltensperger, D., Barrett, M., Blumenthal, J., Bonos, S., Bouton, J., Bransby, D.I., Brummer, C., Burks, P.S., Chen, C., Daly, C., Egenolf, J., Farris, R.L., Fike, J.H., Gaussoin, R., Gill, J.R., Gravois, K., Halbleib, M.D., Hale, A., Hanna, W., Harmoney, K., Heaton, E. A., Heiniger, R.W., Hoffman, L., Hong, C.O., Kakani, G., Kallenbach, R., Macoon, B., Medley, J.C., Missaoui, A., Mitchell, R., Moore, K.J., Morrison, J.I., Odvody, G.N., Richwine, J.D., Ogoshi, R., Parrish, J.R., Quinn, L., Richard, E., Rooney, W.L., Rushing, J.B., Schnell, R., Sousek, M., Staggenborg, S.A., Tew, T., Uehara, G., Viands, D.R., Voigt, T., Williams, D., Williams, L., Wilson, L.T., Wycislo, A., Yang, Y., Owens, V., 2018. Biomass production of herbaceous energy crops in the United States: field trial results and yield potential maps from the multiyear regional feedstock partnership. GCB Bioenergy 10, 698–716. https://doi.org/10.1111/gcbb.12493.

Lee, M.-S., Wycislo, A., Guo, J., Lee, D.K., Voigt, T., 2017. Nitrogen fertilization effects on biomass production and yield components of Miscanthus ×giganteus. Front. Plant Sci. 8. https://doi.org/10.3389/fpls.2017.00544.

Lewandowski, I., Clifton-Brown, J.C., Scurlock, J.M.O., Huisman, W., 2000. Miscanthus: European experience with a novel energy crop. Biomass. Bioenergy 19, 209–227. https://doi.org/10.1016/S0961-9534(00)00032-5.

Lim, S.-H., Yook, M.-J., Song, J.-S., Kim, J.-W., Zhang, C.-J., Kim, D.-G., Park, Y.-H., Lee, D., Kim, D.-S., 2021. Diversity in phenological and agronomic traits of miscanthus sinensis collected in Korea and Eastern Asia. Agronomy 11, 900. https://doi.org/10.3390/agronomy11050900.

Liu, P., Yin, B., Liu, X., Gu, L., Guo, J., Yang, M., Zhen, W., 2023. Optimizing plant spatial competition can change phytohormone content and promote tillering, thereby improving wheat yield. Front. Plant Sci. 14. https://doi.org/10.3389/fpls.2023.1147711.

Maughan, M., Bollero, G., Lee, D.K., Darmody, R., Bonos, S., Cortese, L., Murphy, J., Gaussoin, R., Sousek, M., Williams, D., Williams, L., Miguez, F., Voigt, T., 2012. *M iscanthus* × *giganteus* productivity: the effects of management in different environments. GCB Bioenergy 4, 253–265. https://doi.org/10.1111/j.1757-1707.2011.01144.x.

Miguez, F.E., Villamil, M.B., Long, S.P., Bollero, G.A., 2008. Meta-analysis of the effects of management factors on Miscanthus×giganteus growth and biomass production. Agric. For. Meteorol. 148, 1280–1292. https://doi.org/10.1016/j.agrformet.2008.03.010.

Namoi, N., Jang, C., Behnke, G.D., Lee, J.W., Yang, W., Lee, D., 2024. Nitrogen fertilization effects on aged *Miscanthus* × *giganteus* stands: Exploring biomass yield, yield components, and biomass prediction using in-season morphological traits. GCB Bioenergy 16, e13139. https://doi.org/10.1111/gcbb.13139.

Namoi, N., Jang, C., Robins, Z., Lin, C.-H., Lim, S.-H., Voigt, T., Lee, D., 2022. Aerial imagery can detect nitrogen fertilizer effects on biomass and stand health of Miscanthus × giganteus. Remote Sens. 14, 1435. https://doi.org/10.3390/rs14061435.

Namoi, N., Jang, C., Voigt, T., Lee, D., 2026. Soil fertility management for sustainable *Miscanthus* × *giganteus* production: Increased tiller weight from nitrogen management explains yield gains in aged miscanthus. Biomass. Bioenergy 204, 108394. https://doi.org/10.1016/j.biombioe.2025.108394.

Njuguna, J.N., Clark, L.V., Anzoua, K.G., Bagmet, L., Chebukin, P., Dwiyanti, M.S., Dzyubenko, E., Dzyubenko, N., Ghimire, B.K., Jin, X., Johnson, D.A., Jørgensen, U., Kjeldsen, J.B., Nagano, H., Peng, J., Petersen, K.K., Sabitov, A., Seong, E.S., Yamada, T., Yoo, J.H., Yu, C.Y., Zhao, H., Long, S.P., Sacks, E.J., 2023. Biomass yield in a genetically diverse Miscanthus sacchariflorus germplasm panel phenotyped at five locations in Asia, North America, and Europe. GCB Bioenergy 15, 642–662. https://doi.org/10.1111/gcbb.13043.

Ouattara, M.S., Laurent, A., Barbu, C., Berthou, M., Borujerdi, E., Butier, A., Malvoisin, P., Romelot, D., Loyce, C., 2020. Effects of several establishment modes of *Miscanthus* × *giganteus* and *Miscanthus sinensis* on yields and yield trends. GCB Bioenergy 12, 524–538. https://doi.org/10.1111/gcbb.12692.

Robson, P., Jensen, E., Hawkins, S., White, S.R., Kenobi, K., Clifton-Brown, J., Donnison, I., Farrar, K., 2013. Accelerating the domestication of a bioenergy crop: identifying and modelling morphological targets for sustainable yield increase in Miscanthus. J. Exp. Bot. 64, 4143–4155. https://doi.org/10.1093/jxb/ert225.

Sanderson, M.A., Reed, R.L., 2000. Switchgrass growth and development: Water, nitrogen, and plant density effects. J. RANGE Manag.

Sharma, B.P., Zhang, N., Lee, D., Heaton, E., Delucia, E.H., Sacks, E.J., Kantola, I.B., Boersma, N.N., Long, S.P., Voigt, T.B., Khanna, M., 2022. Responsiveness of miscanthus and switchgrass yields to stand age and nitrogen fertilization: a meta-regression analysis. GCB Bioenergy 14, 539–557. https://doi.org/10.1111/gcbb.12929.

Studt, J.E., McDaniel, M.D., Tejera, M.D., VanLoocke, A., Howe, A., Heaton, E.A., 2021. Soil net nitrogen mineralization and leaching under *Miscanthus* × *giganteus* and *Zea mays*. GCB Bioenergy 13, 1545–1560. https://doi.org/10.1111/gcbb.12875.

Tejera, M., Boersma, N.N., Archontoulis, S.V., Miguez, F.E., VanLoocke, A., Heaton, E.A., 2022. Photosynthetic decline in aging perennial grass is not fully explained by leaf nitrogen. J. Exp. Bot. 73, 7582–7595. https://doi.org/10.1093/jxb/erac382.

Tejera, M., Boersma, N., Vanloocke, A., Archontoulis, S., Dixon, P., Miguez, F., Heaton, E., 2019. Multi-year and multi-site establishment of the perennial biomass crop miscanthus × giganteus using a staggered start design to elucidate N response. Bioenerg. Res. 12, 471–483. https://doi.org/10.1007/s12155-019-09985-6.

Tejera, M.D., Miguez, F.E., Heaton, E.A., 2021. The older plant gets the sun: age-related changes in *Miscanthus* × *giganteus* phenology. GCB Bioenergy 13, 4–20. https://doi.org/10.1111/gcbb.12745.

U.S. Department of Energy, 2021. Memorandum of Understanding: Sustainable Aviation Fuel Grand Challenge.

U.S. Department of Energy, 2024. Langholtz, M. H. (Ed.), 2023 Billion-Ton Report: An Assessment of U.S. Renewable Carbon Resources. Ridge National Laboratory, Oak Ridge, TN: Oak. doi:10.23720/BT2023/2316165.

U.S. Department of Energy; U.S. Department of Transportation; U.S. Department of Agriculture, 2022. Sustainable Aviation Fuel Grand Challenge Roadmap: Flight Plan for Sustainable Aviation Fuel Report.

VanLoocke, A., Twine, T.E., Zeri, M., Bernacchi, C.J., 2012. A regional comparison of water use efficiency for miscanthus, switchgrass and maize. Agric. For. Meteorol. 164, 82–95. https://doi.org/10.1016/j.agrformet.2012.05.016.

Vermerris, W., 2008. Miscanthus: Genetic Resources and Breeding Potential to Enhance Bioenergy Production. In: Vermerris, W. (Ed.), Genetic Improvement of Bioenergy Crops. Springer New York, New York, NY, pp. 295–308. https://doi.org/10.1007/978-0-387-70805-8_10.

Villalobos, F.J., Fereres, E. (Eds.), 2016. Principles of Agronomy for Sustainable Agriculture. Springer International Publishing, Cham. https://doi.org/10.1007/978-3-319-46116-8.

Xue, S., Kalinina, O., Lewandowski, I., 2015. Present and future options for Miscanthus propagation and establishment. Renew. Sustain. Energy Rev. 49, 1233–1246. https://doi.org/10.1016/j.rser.2015.04.168.

Yang, C., Li, L., 2017. Hormonal regulation in shade avoidance. Front. Plant Sci. 8. https://doi.org/10.3389/fpls.2017.01527.

Zhou, J., Hua, Z., Zhang, Y., Li, Z., Xu, S., Tian, X., Dong, H., Li, Z., 2025. Light-hormone crosstalk modulates vegetative branching and yield stability in dual-planting cotton systems. Field Crops Res. 333, 110103. https://doi.org/10.1016/j.fcr.2025.110103.

Zhou, J., Nie, J., Kong, X., Dai, J., Zhang, Y., Zhang, D., Cui, Z., Hua, Z., Li, Z., Dong, H., 2023. Cotton yield stability achieved through manipulation of vegetative branching and photoassimilate partitioning under reduced seedling density and double seedlings per hole. Field Crops Res. 303, 109117. https://doi.org/10.1016/j.fcr.2023.109117.